EM Implosion Memos

Memo 44

May, 2010

The truncated four feed-arm configuration with switch cones (T4FASC) and a cylindrical pressure vessel

Prashanth Kumar, Serhat Altunc, Carl E. Baum, Christos G. Christodoulou and Edl Schamiloglu

University of New Mexico

Department of Electrical and Computer Engineering

Albuquerque, NM 87131

Abstract

In this paper, numerical simulations are used to investigate the truncated four feed-arm configuration with the switch cones (T4FASC) and a cylindrical pressure vessel. The near-field electric field responses and the focal impulse waveforms are compared to the T4FASC-CSS-SPVSHC and T4FASC-CSS-SPVCHC designs in [1]. The peak focal impulse amplitudes for various pressure vessel radii are compared to validate the calculations in [2].

1 Introduction

The T4FASC-CSS-SPVSHC configuration has been demonstrated to be the most promising of all the switch and pressure vessel designs investigated so far [1, 3]. This paper explores the T4FASC-CSS with a cylindrical pressure vessel and cylindrical hydrogen chamber (CPVCHC) as per analytical calculations outlined in [2]. The T4FASC-CSS-CPVCHC is particularly attractive due to its ease-of-fabrication.

2 Setup

Using the formulas in [2], the pressure vessel dimensions are calculated so that the surrounding oil medium can be used as the launching lens.

2.1 Structure visualization

Figure 2.1 shows the perspective view of the T4FASC-CSS with the CPVCHC and the reflector. The details of the switch geometry are shown in Fig. 2.2.
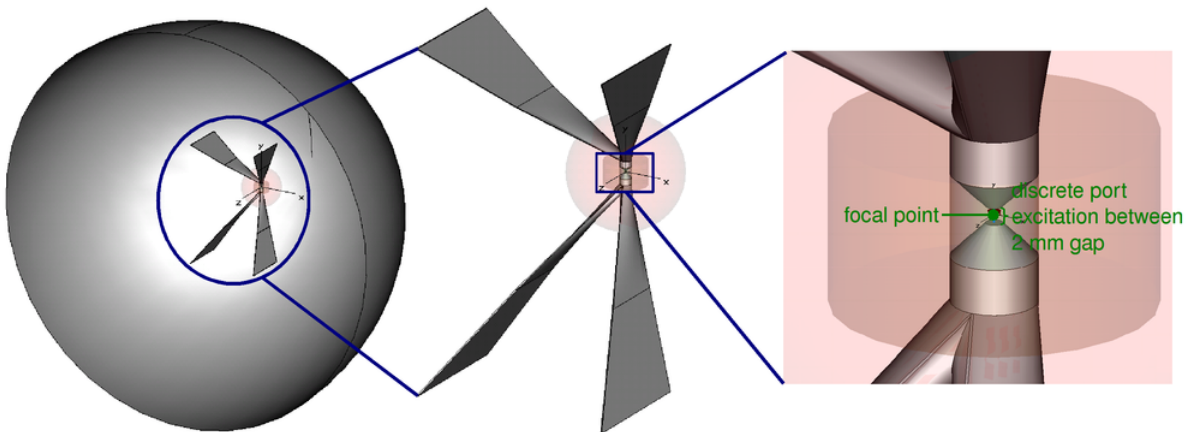

Figure 2.1: Perspective view of T4FASC-CSS-CPVCHC configuration with reflector; "Zoomed-in" view showing CPVCHC and discrete port excitation.

The dimensions of the switch system components are summarized in Table 1. The radius and height of the pressure vessel are determined using the formulas in [2] for $r_{\mathrm{hc}} = h \tan \theta = 0.5 \tan(45.58°) = 0.51$ cm and $\epsilon_{r_{ll}} = 2.25$. Also, $h_{\mathrm{pv}} = h + H_{\mathrm{css}}$.

3 CST parameters

- CST parameters and probe placements are identical to those in [4].

- In all simulations, a discrete port, 1 V, 100 ps, ramp rising step, excitation is applied between a 2 mm gap in the switch cones.
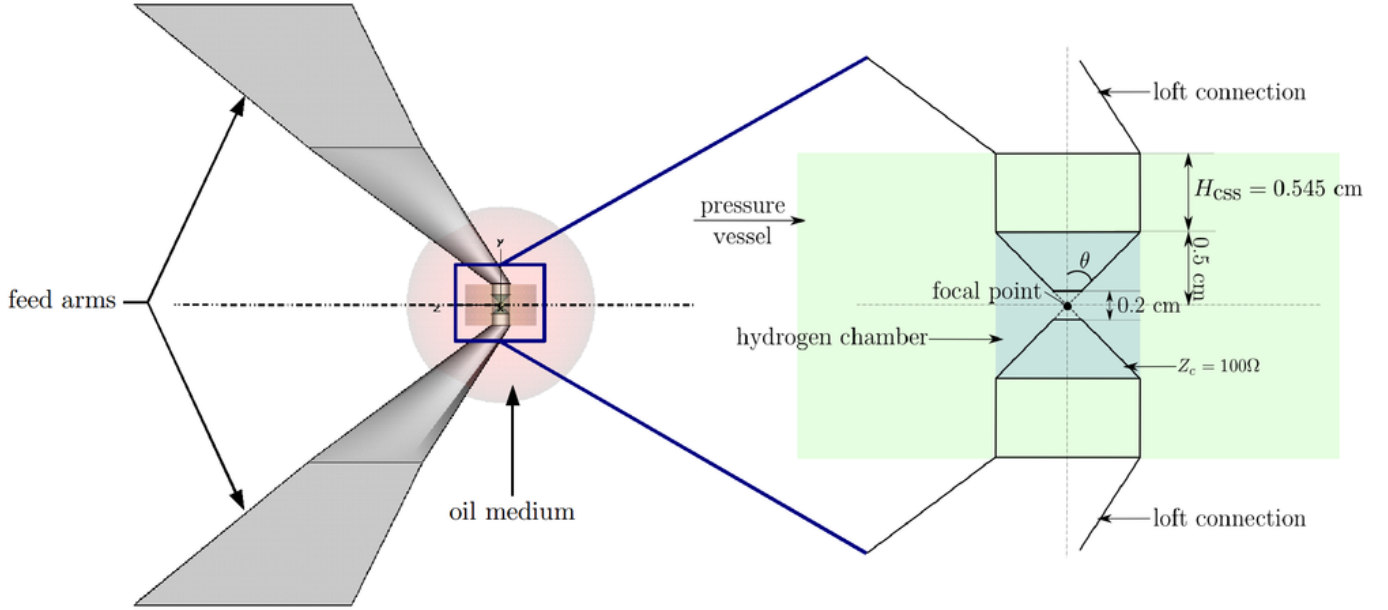
Figure 2.2: Geometrical details and "zoomed-in" side view of switch system for the T4FASC-CSS-CPVCHC configuration.

Table 1: Dimensions of switch system components

| Component	Height (cm)	Radius (cm)
switch cone	$h = 0.5$	$r = h\tan\theta$
cylindrical support	$H_{\text{css}} = 0.545$	$r = h\tan\theta$
hydrogen chamber	$h_{\text{hc}} = 1.0$	$r_{\text{hc}} = h\tan\theta$
pressure vessel	$h_{\text{pv}} = 1.045$	$r_{\text{pv}} = 1.905$
oil medium	–	$r_{\text{oil}} = 5.0$

4 Results

Normalized responses from the electric field probes given in Appendix-I (each response is normalized with respect to its maximum). As expected, the E_ϕ component in the $-yz$-plane and the E_θ component in the $-zx$-plane are zero. The E_θ component in the xy-plane has a time spread $\lesssim 25$ ps. The time spread observed in the E_ϕ component in the $xy-$plane is < 15 ps. The largest time spread, ≈ 35 ps, is observed in the E_θ component in the $-yz$-plane. The E_ϕ component in the $-zx$-plane has a time spread $\lesssim 20$ ps.

The focal waveform and the beam width (spot size) are shown in Fig. 4.1. The peak impulse amplitude is 11.701 V/m, the beam width (spot size) is 4.949 cm and ΔFWHM is 19.587 ps. Although the spot size and ΔFWHM are similar to the bicone configurations [3], the larger peak impulse amplitude makes this design practically more attractive.

3
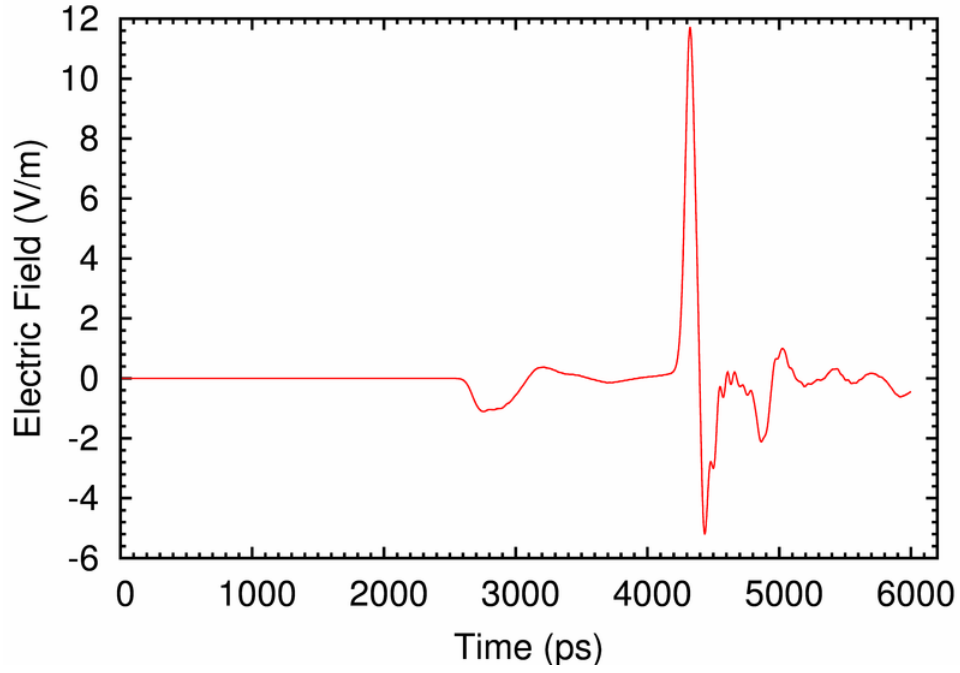
(a) Focal impulse waveform.
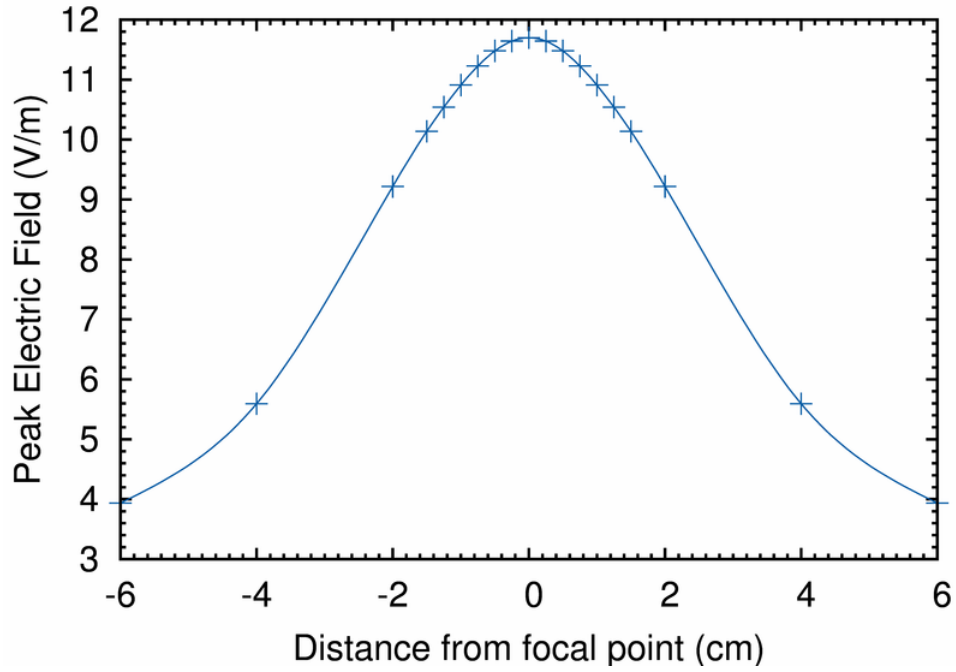
(b) Beam width.

Figure 4.1: Focal impulse waveform and beam width for the T4FASC-CSS-CPVCHC configuration.

Validation of analytical calculations in [2]

To validate the analytical calculations in [2], the peak focal impulse amplitude ($E_{\max}$), ΔFWHM, and beam width for various r_{pv} and $\epsilon_{r_{\mathrm{oil}}}$ are tabulated in Table 2. The height of the pressure vessel

is fixed, $h_{\mathrm{pv}} = 1.045$ cm. The first row in the table corresponds to results from Fig. 4.1.

Table 2: Comparison of peak $E_{\max}$, ΔFWHM and beam width for various r_{pv} and $\epsilon_{r_{\mathrm{oil}}}$

PV parameters				
r_{pv} (cm)	$\epsilon_{r_{\mathrm{oil}}}$	$E_{\max}$ (V/m)	ΔFWHM (ps)	Beam width (cm)
1.905	2.25	11.701	19.587	4.949
1.0	2.25	11.340	20.742	5.080
4.0	2.25	11.696	20.699	4.875
1.905	9.0	8.931	34.483	5.702
0.75	9.0	10.241	26.789	5.376

The r_{pv} and $\epsilon_{r_{\mathrm{oil}}}$ values in rows 2-5 are arbitrary, i.e., they are not obtained from the equations in [2]. Therefore, for these values, one would expect large deviations in the $E_{\max}$ and spot size compared to the first row. Clearly this is not the case. This inconsistancy can be explained as follows,

1. The high-frequency (optical) approximations used in [2] are inaccurate for determining the dimensions of the pressure vessel since they do not take into account the lower frequencies (larger wavelengths) in the input pulse.

2. The hydrogen chamber does not play *any* role in the propagation of the expanding spherical wave.

The second point can be partly explained using the analytical procedure in [2]. Consider Fig. 4.2, reproduced from [2]. If one assumes that $\epsilon_{r_{ll}} = \epsilon_{r_{\mathrm{oil}}}$, and $\epsilon_{r_{\mathrm{hc}}} = \epsilon_{r_{\mathrm{pv}}}$, i.e., the hydrogen chamber is ignored, the equal time condition, with a 10 ps tolerance, for a wave originating at the focal point is,

$$\left| \frac{OB\sqrt{\epsilon_{r_{\mathrm{pv}}}} - OC'\sqrt{\epsilon_{r_{\mathrm{pv}}}} - C'C\sqrt{\epsilon_{r_{\mathrm{oil}}}}}{c} \right| \leq 10 \text{ ps} \tag{4.1}$$

$$\Rightarrow \left| \frac{\sqrt{\epsilon_{r_{\mathrm{pv}}}}\sqrt{r_{\mathrm{pv}}^2 + h_{\mathrm{pv}}^2} - r_{\mathrm{pv}}\sqrt{\epsilon_{r_{\mathrm{pv}}}} - (r_{ll} - r_{\mathrm{pv}})\sqrt{\epsilon_{r_{\mathrm{oil}}}}}{c} \right| \leq 10 \text{ ps}$$

$$\Rightarrow \left| \frac{\sqrt{\epsilon_{r_{\mathrm{pv}}}}\sqrt{r_{\mathrm{pv}}^2 + h_{\mathrm{pv}}^2} - r_{\mathrm{pv}}\sqrt{\epsilon_{r_{\mathrm{pv}}}} - (\sqrt{r_{\mathrm{pv}}^2 + h_{\mathrm{pv}}^2} - r_{\mathrm{pv}})\sqrt{\epsilon_{r_{\mathrm{oil}}}}}{c} \right| \leq 10 \text{ ps}$$

where c is the speed of light. Therefore the condition is,

$$\xi \text{ (say)} = \left| \frac{[\sqrt{\epsilon_{r_{\mathrm{pv}}}} - \sqrt{\epsilon_{r_{\mathrm{oil}}}}][\sqrt{r_{\mathrm{pv}}^2 + h_{\mathrm{pv}}^2} - r_{\mathrm{pv}}]}{c} \right| \leq 10 \text{ ps} \tag{4.2}$$

Table 3 shows ξ values obtained by applying equation (4.2) to the various r_{pv} and $\epsilon_{r_{\mathrm{oil}}}$ values in Table 2.
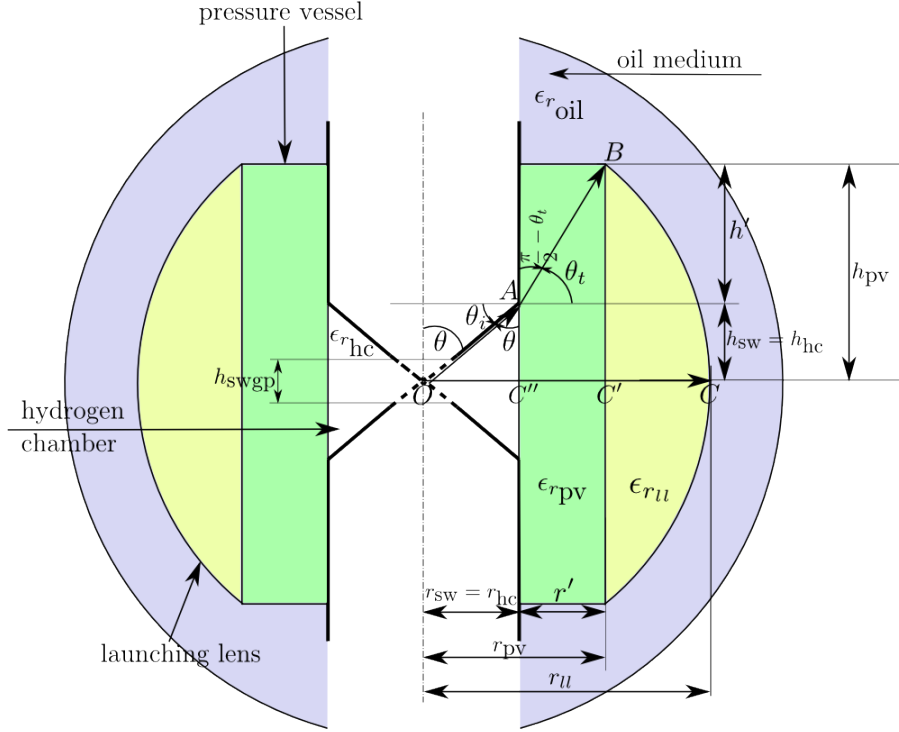
Figure 4.2: Diagram for cylindrical pressure vessel and launching lens calculations.

Table 3: Equation (4.2) for various r_{pv} and $\epsilon_{r_{\mathrm{oil}}}$

r_{pv} (cm)	$\epsilon_{r_{\mathrm{oil}}}$	ξ (ps)
1.905	2.25	3.78
1.0	2.25	6.30
4.0	2.25	1.90
1.905	9.0	9.61
0.75	9.0	19.24

One observes that the ξ values in Table 3 are consistent with observations in Table 2, i.e., to first order, $E_{\max} \propto \xi^{-1}$ and (spot size) $\propto \xi$. Hence Table 3 shows, at least for the high frequencies in the input pulse, that the hydrogen chamber is "ignored" by the outward propagating spherical wave.

Plots for all the results in Table 2 are given in Appendix-II.

5   Conclusion

The peak focal impulse amplitude is greater than the bicone configurations in [3] and of the same order as the T4FASC-CSS-SPVCHC design in [1]. However, the ease-of-fabrication of the

CPVCHC makes it very attractive for experimental investigation. It has also been shown that,

1. The optical approximations used to determine the height of the pressure vessel and $\epsilon_{r_{ll}}$ in [2] are inaccurate as the larger wavelengths in the input pulse are not taken into account.

2. The hydrogen chamber can be ignored in the analysis of the problem.

References

[1] Prashanth Kumar, Carl E. Baum, Serhat Altunc, Christos G. Christodoulou and Edl Schamiloglu, "The truncated four feed-arm configuration with switch cones (T4FASC) and a spherical pressure vessel." EM Implosion Memo 42, May 2010.

[2] Prashanth Kumar, Carl E. Baum, Serhat Altunc, Christos G. Christodoulou and Edl Schamiloglu, "Design considerations for a cylindrical pressure vessel with a spherical launching lens." EM Implosion Memo 40, Mar. 2010.

[3] Prashanth Kumar, Carl E. Baum, Serhat Altunc, Christos G. Christodoulou and Edl Schamiloglu, "150 ω impedance-matched bicone switch configuration with a spherical pressure vessel."

[4] Prashanth Kumar, Carl E. Baum, Serhat Altunc, Christos G. Christodoulou and Edl Schamiloglu, "Effect of the impedance of a bicone switch on the focal impulse amplitude and beam width." EM Implosion Memo 38, Feb. 2010.

APPENDIX-I

Normalized E_θ and E_ϕ electric field components.
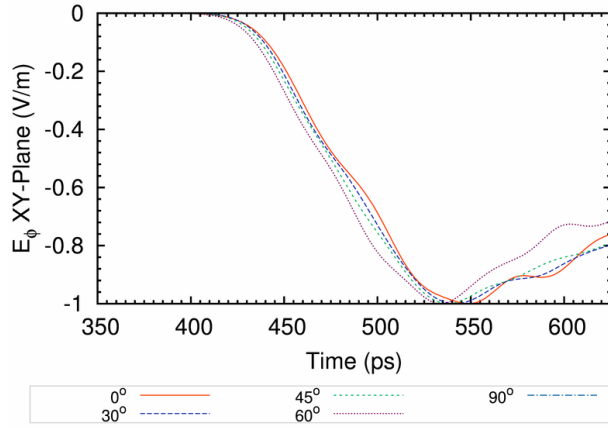
(a) Normalized E_ϕ in the $xy-$plane
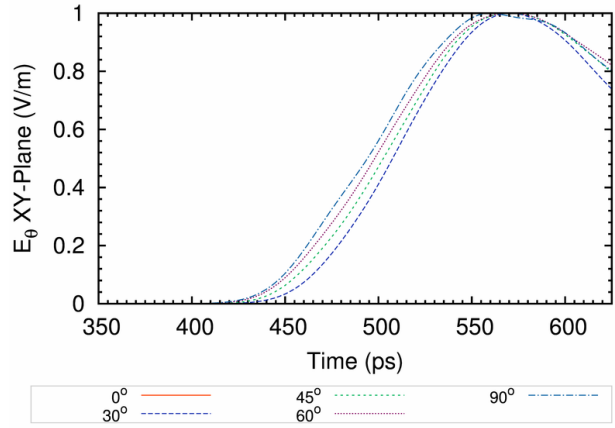
(b) Normalized E_θ in the $xy-$plane
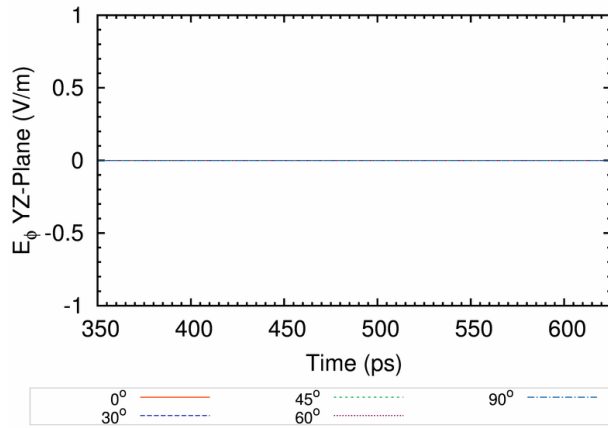
(c) Normalized E_ϕ in the $-yz-$plane
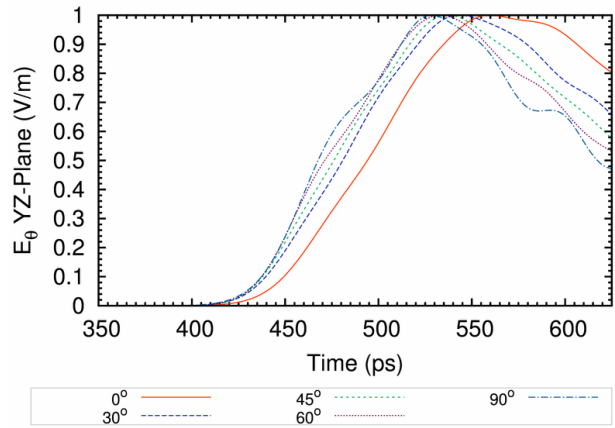
(d) Normalized E_θ in the $-yz-$plane
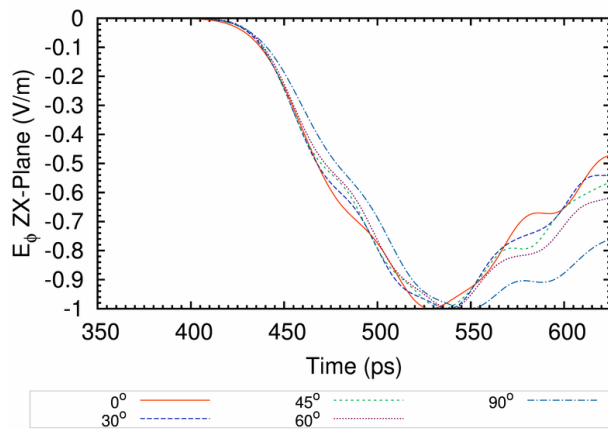
(e) Normalized E_ϕ in the $-zx-$plane
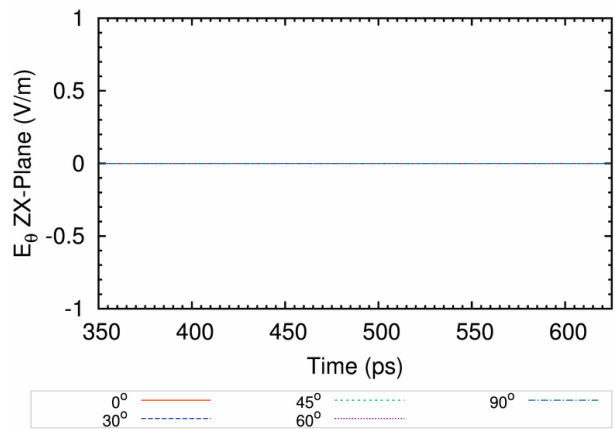
(f) Normalized E_θ in the $-zx-$plane

Figure 5.1: Normalized E_θ and E_ϕ components of the responses from the electric field probes on the $xy, -yz$ and $-zx$ planes.

Appendix-II

Focal impulse waveforms and beam widths for the various pressure vessel radii, r_{pv}, and oil permittivity, $\epsilon_{r_{\mathrm{oil}}}$.
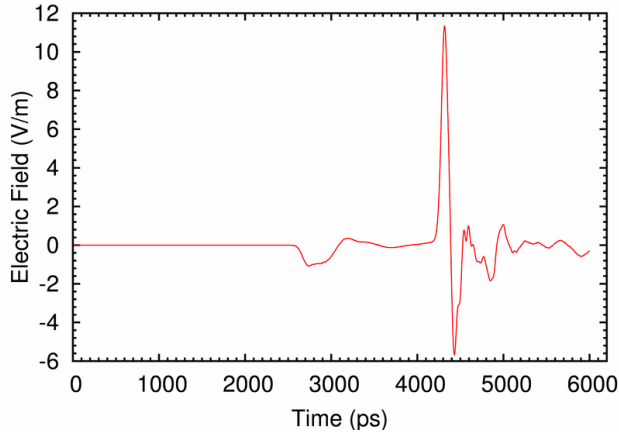
(a) Focal impulse waveform for $r_{\mathrm{pv}} = 1.0$ cm and $\epsilon_{r_{\mathrm{oil}}} = 2.25$
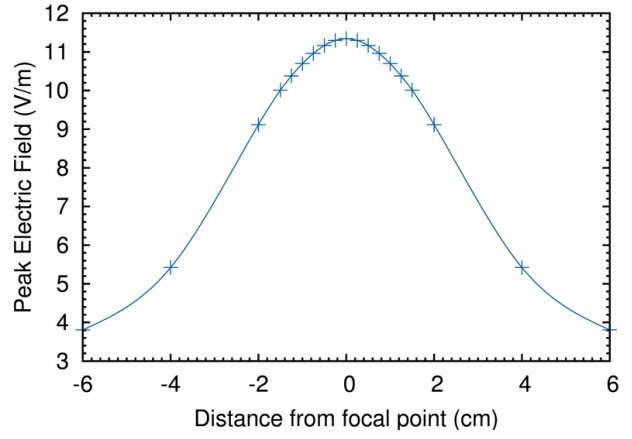
(b) Spot size for $r_{\mathrm{pv}} = 1.0$ cm and $\epsilon_{r_{\mathrm{oil}}} = 2.25$
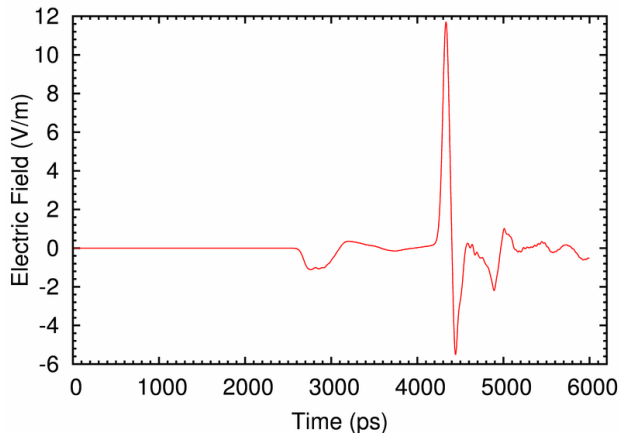
(c) Focal impulse waveform for $r_{\mathrm{pv}} = 4.0$ cm and $\epsilon_{r_{\mathrm{oil}}} = 2.25$
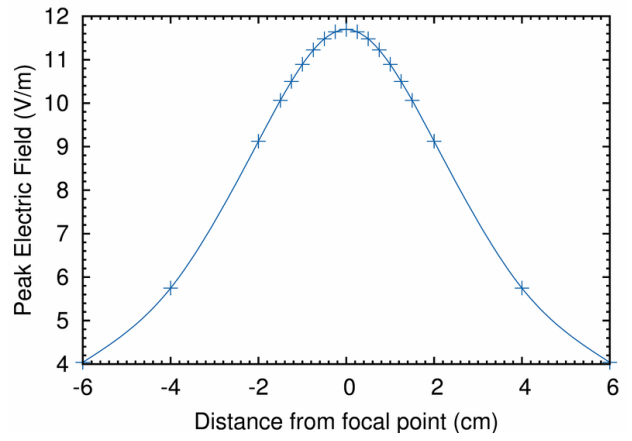
(d) Spot size for $r_{\mathrm{pv}} = 4.0$ cm and $\epsilon_{r_{\mathrm{oil}}} = 2.25$

Figure 5.2: Focal impulse waveform and beam width for various pressure vessel radii, r_{pv}, .
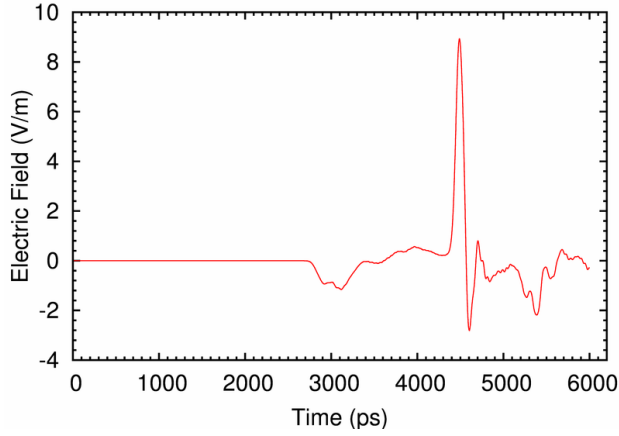
(a) Focal impulse waveform for $r_{pv} = 1.905$ cm and $\epsilon_{r_{oil}} = 9.0$
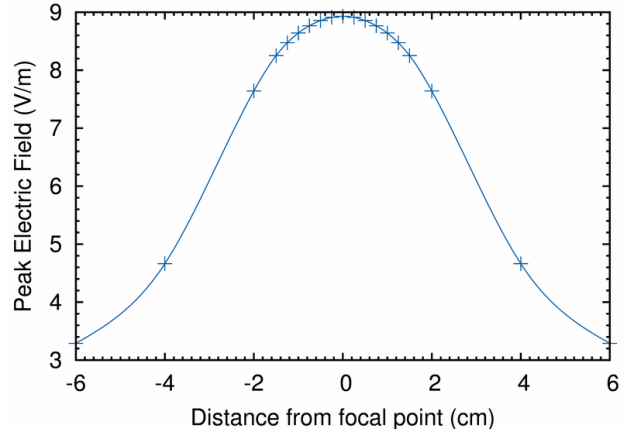
(b) Spot size for $r_{pv} = 1.905$ cm and $\epsilon_{r_{oil}} = 9.0$
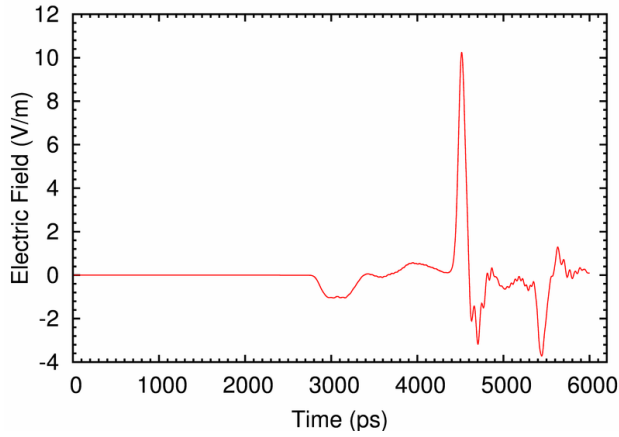
(c) Focal impulse waveform for $r_{pv} = 0.75$ cm and $\epsilon_{r_{oil}} = 9.0$
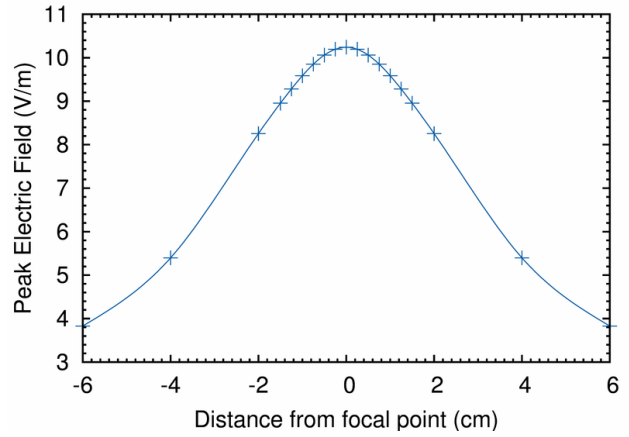
(d) Spot size for $r_{pv} = 0.75$ cm and $\epsilon_{r_{oil}} = 9.0$

Figure 5.3: Focal impulse waveform and beam width for various pressure vessel radii, r_{pv}, and oil permittivity, $\epsilon_{r_{oil}}$. .